

Unveiling the formation route of the largest galaxies in the Universe

Jaime D. Perea¹★ and José M. Solanes²★

¹*Instituto de Astrofísica de Andalucía, IAA-CSIC. Glorieta de la Astronomía, s/n; E-18008 Granada, Spain*

²*Departament de Física Quàntica i Astrofísica and Institut de Ciències del Cosmos (ICCUB), Universitat de Barcelona. C. Martí i Franquès, 1; E-08028 Barcelona, Spain*

Accepted 2016 May 30. Received 2016 May 30; in original form 2015 September 2

ABSTRACT

Observational evidence indicates that the role of gas is secondary to that of gravity in the formation of the most luminous spheroids inhabiting the centres of galaxy associations, as originally conjectured in the late 80s/early 90s. However, attempts to explain the origin of the Fundamental Plane (FP) of massive early-type galaxies (ETGs) – a tilted version of the scaling relation connecting the size, velocity dispersion and mass of virialized homologous systems – based on sequences of pairwise mergers, have systematically concluded that dissipation cannot be ignored. We use controlled simulations of the pre-virialization stage of galaxy groups to show that multiple collisionless merging is capable of creating realistic first-ranked galaxies. Our mock remnants define a thin FP that perfectly fits data from all kinds of giant ETGs in the local volume, showing the existence of a unified relationship for these systems. High-ranked galaxies occupy in the FP different areas than standard objects, a segregation which is viewed essentially as zero-point offsets in the 2D correlations arising from standard projections of this plane. Our findings make a strong case for considering hierarchical dissipationless merging a viable route for the formation of the largest galaxies in the Universe.

Key words: galaxies: elliptical and lenticular, cD – galaxies: formation – galaxies: fundamental parameters – galaxies: groups: general – galaxies: interactions – galaxies: kinematics and dynamics.

1 THE MERGERS-MAKE-ELLIPTICALS HYPOTHESIS

The possibility that ellipticals form by mergers of two or more pre-existing galaxies, typically discs, was first suggested by Toomre (1977) as an alternative to the top-down monolithic collapse hypothesis (Eggen, Lynden-Bell & Sandage 1962). That was some years before cosmological observations start to point heavily to a world model in which galaxies form within an underlying structure built up hierarchically through the collapse and subsequent merger of cold dark matter (CDM) haloes. It was precisely this generic feature of CDM models, the continuous bottom-up growth of structure in all scales – nearly unabated until recently ($z \lesssim 0.5$) when the Universe has entered a phase of dark energy domination – that provided important clues to alleviate the first objections raised by early simulations of the merger scenario. In those days, numerical models mostly focused on pairwise collisions of similar stellar discs, producing remnants that rotated too fast and had ellipticities that were too large to represent true massive ellipticals. The addition of an extended CDM component around the colliding galaxies facilitated the transfer of the orbital angular momentum deposited in

the discs along the merger to the common dark halo, thus reducing the rotation speed of the final stellar remnant to values consistent with observations. Moreover, it soon became clear that understanding the formation of early-type galaxies (ETGs) demanded repeated mergers of progenitors covering a wide range of masses (e.g. Shen et al. 2003; Ciotti, Lanzoni & Volonteri 2007; Trujillo, Ferreras & de La Rosa 2011; Moody et al. 2014). Multiple merging led to the formation of oblate-triaxial, and therefore more rounder-looking, remnants (Weil & Hernquist 1996).

Another important obstacle to the merger hypothesis is the necessity of building objects exhibiting central light distributions more concentrated than those of their most likely progenitors. As stated by Carlberg (1986), the macroscopic phase space densities of the cores of intermediate- and low-luminosity elliptical galaxies are found to generally exceed the phase space densities measured in galactic discs. Since according to Liouville’s theorem the phase space probability in a dynamically reversible system must be kept constant, this argues against the formation of the bulk of the elliptical population via collisionless mergers of stellar discs, a point also stressed by Ostriker (1980) soon after the merger hypothesis was formulated. To overcome this problem Carlberg suggested dealing with mergers of spirals that either include a high-mass density spheroidal component (e.g. a bulge), or are largely gaseous and thus capable of introducing irreversibility in the system by effectively

* E-mail: jaime@iaa.es (JDP); jm.solanes@ub.edu (JMS)

dissipating part of the energy deposited into the core. The fact that the central space densities of ellipticals depend strongly on luminosity ($\propto L_B^{-2.35}$ as estimated by Carlberg 1986) turned dissipative merging into an alternative that was worth exploring.

Using a large suite of simulations of equal-mass mergers of discs, both with and without gas, Robertson et al. (2006) (see also Hopkins, Cox & Hernquist 2008), showed that dissipation imprints a mass-dependent relation in the ratio of total mass to stellar mass of the remnants of the form

$$\frac{M}{M_*} \propto M_*^\gamma. \quad (1)$$

This relationship arises from the halo mass dependence of the cooling efficiency of the intergalactic medium (IGM) collisionally heated during the merger. In gas-rich low-mass systems the hot intergalactic gas cools rapidly producing inflows giving rise to a central merger induced starburst that is compact. However, in a wet merger between two large spirals the IGM cannot cool efficiently and remains in the halo for the duration of the merger, causing more massive galaxies to act increasingly as dissipationless systems. This produces low- and intermediate-mass final remnants that are more baryon dominated in their central regions than their more massive counterparts, giving rise to a dependence of the form (1) with γ small ($\sim 0.1-0.2$) but positive,¹ as found in some observational studies (e.g. Padmanabhan et al. 2004).

It is straightforward to show, provided $R \propto M_*^\mu$, that equation (1) can be transformed into the power-law relation

$$R \propto (\sigma^2 I^{-1})^\lambda, \quad (2)$$

with $I \propto M_*/R^2$, R the projected radius of the system, σ its line-of-sight velocity dispersion² and

$$\lambda = \left(\frac{\gamma}{\mu} + 1 \right)^{-1}, \quad (3)$$

an index measuring the ‘tilt’ relative to the standard plane, $R \propto \sigma^2 I^{-1}$, that arises when one assumes for virialized remnants baryon fraction invariance and structural and dynamical homology. The most useful version of equation (2) is none the less a generalization that accounts for either non-homology, or variations in the stellar mass fraction, or both, and that replaces M_*/R^2 by a directly measurable property such as the surface brightness μ . If we transform this new expression by dividing it by R^2 and taking logarithms, solving for R we get

$$\log R = a \log \sigma + b(\mu/2.5) + c. \quad (4)$$

In this case the tilt is expressed in slope coefficients that differ from the standard values: $a = 2$ and $b = 1$. Equation (4) defines what is known as the Fundamental Plane (FP) of elliptical galaxies, a scaling between the three global properties of mass – implicit in the stellar surface brightness – size, and velocity dispersion (or specific internal energy) that shape up the pivotal space (hereafter the *RVM* space) in which to study galaxies of all kinds (see e.g. Darriba & Solanes 2010; Toribio et al. 2011; Bezanson, Franx & van

Dokkum 2015, and references therein).³ Introduced by Djorgovski & Davis (1987) and Dressler et al. (1987) as a precise distance indicator for ETGs, the widely studied FP of ellipticals combines the two well-known 2D Faber–Jackson $L-\sigma$ relation (FJR; Faber & Jackson 1976) and $R-\mu$ relation (Kormendy 1977) into a 3D scaling in *RVM* space with a yet more reduced scatter (< 0.1 dex in the perpendicular direction). Both the tilt and tightness of this plane are used as powerful constraints on theoretical models of ETG formation.

Robertson et al. (2006) also demonstrated that for sufficiently high gas fractions ($f_{\text{gas}} \geq 0.4$) the remnants of pairwise mergers can yield a simulated FP with nearly the same tilt ($\lambda \sim 0.75$) observed in the NIR (see e.g. the recent results by La Barbera et al. 2010; values quoted in the literature, however, may vary with wavelength, environment and redshift). In the same way, gas-rich dissipational simulations produce model $R-M_*$ relations with a slope ($\mu \simeq 0.55$) that compares well with the relation measured for nearby ETGs (e.g. Shen et al. 2003; Huertas-Company et al. 2013), and that is fully consistent with the formula (3) given the previously quoted values of λ and γ . Further analysis of these sort of simulations by Cox et al. (2006) and Hoffman et al. (2010) showed that an increase in the gas fraction produced remnants progressively more oblate and rounder, that rotate faster and that, in general, match far better than their dissipationless counterparts the 1D and 2D structural and kinematic properties of ~ 80 per cent of the nearby ETGs observed in integral-field spectroscopic surveys (Emsellem et al. 2007). However, the same dissipational merger simulations that successfully reproduced the observed properties of low- and intermediate-mass ellipticals, had trouble explaining the formation of luminous, non-rotating spheroids, with old stars, shallow cusps and boxy isophotes, which make the remaining 20 per cent of the local ETG population (Novak 2008; Moody et al. 2014). On the other hand, now a growing body of evidence, both theoretical (e.g. Shen et al. 2003) and observational (e.g. Bernardi et al. 2007; Liu et al. 2008; Beifiori et al. 2014), indicates that the mass growth of the largest ellipticals, especially the brightest members of groups and clusters, is quite likely driven by a sequence of (gradually minor) dissipationless mergers, the role of gas being restricted at most to very early epochs (e.g. De Lucia & Blaizot 2007; Oser et al. 2010). More interesting still, is the fact that first-ranked galaxies define essentially the same FP of their less massive counterparts, although with an even smaller scatter (e.g. Bernardi et al. 2007; Liu et al. 2008). This reduced dispersion is also in agreement with a dry merger formation history.

All these findings are consistent with the idea, advanced many years before by Kormendy (1989) and Bender, Burstein & Faber (1992), that the importance of gas during the merger process declines with galaxy mass. This hypothesis, which Bender et al. (1992) embodied in the concept of *merging continuum*, seems none the less to be in conflict with the outcome of most galaxy merger experiments. In many of these simulations the tilt of the FP is exclusively driven by gas dissipation, with the role of gravity being limited to the preservation of the slope created by the gas (e.g. Nipoti, Londrillo & Ciotti 2003; Robertson et al. 2006). If this were the case, then the tilted FP of first-ranked galaxies in the local Universe, which as observations suggest are essentially composed of very old stars (formed at $z > 2$), would be a legacy from at least ~ 10 billion

¹ The evidence supporting a positive slope for the elliptical population is still controversial, especially from the data recently reported by the ATLAS3D survey (Cappellari et al. 2013).

² In this reasoning we are assuming, for simplicity, sphericity and isotropic orbital structure for the galaxies. For a more general discussion of the FP and its relation with the virial theorem see, for instance, Ciotti (1997) and references therein.

³ The exact definitions of the global variables used in these equations are irrelevant, as long as they refer to quantities that can be related directly to the corresponding properties entering the virial theorem.

years ago. We believe that the root of the problem is that, as mentioned before, both dry and wet pre-prepared merger simulations have traditionally focused on binary collisions, recreating merger hierarchies at best throughout two or three non-overlapping merger steps which use the remnants of the previous one to realize the initial conditions of the next (Dantas et al. 2003; Robertson et al. 2006; Nipoti et al. 2009; Moody et al. 2014). It is quite clear that these idealizations of multiple merging are only gross descriptions of the diversity, in terms of frequencies and mass ratios, of galaxy interactions that shape the brightest ETGs in the course of cosmic evolution.

Pending the study of large sets of brightest members of galaxy systems through full cosmological simulations becomes computationally affordable, the best approach to investigate the assembly and properties of such objects by means of cosmologically consistent merger histories is nowadays through controlled experiments of aggregations of multiple galaxies undergoing gravitational collapse. It is important to focus on groups of galaxies rather than on pairs, because of the necessity of building a dense environment in which galaxies are prone to suffer numerous collisions, whilst dynamically young small-size overdensities provide a framework in which both the frequency and strength of interactions, and therefore the merger likelihood, are maximized. To our knowledge, the only investigation on the role of gravitational dynamics in the formation of massive ETGs conducted along these lines is the recent work by Taranu, Dubinski & Yee (2013, 2015). By studying collapsing groups of 3–25 disc galaxies spanning a range of masses, these authors have demonstrated that multiple dry merging is certainly a plausible route for the formation of the most massive ellipticals. In particular, Taranu et al. (2015) have shown that hierarchical sequences of dissipationless mergers of spiral galaxies can produce first-ranked objects obeying a significantly tilted FP, although somewhat less strongly than observations suggest. In the same way, they have found that this scenario results in exceptionally tight 2D and 3D relationships between the most important physical properties of central remnants.

In the next section, we present a similar experiment to that of Taranu et al. (2013), based on controlled high-resolution numerical simulations of the pre-virialization stage of isolated groups of galaxies, which produces even more striking outcomes regarding the origin of the FP defined by the most massive members of galaxy aggregations (Section 3). Our set-up is somewhat more elaborated than theirs in certain aspects. The main differences in our approach – in which the key of our better performance appears to lie – are the simultaneous inclusion of late- and early-type galaxy models to account for the expected mix of progenitors’ populations; the non-homologous scaling of the progenitors’ global properties; the inclusion of a common dark matter background within which galaxies are randomly distributed; and the scaling of the progenitors’ dark halo masses to values appropriate for the initial redshift of the simulation, which is also significantly higher ($z_i = 3$ versus $z_i = 2$). By contrast, we are more restrictive than Taranu et al. (2013) in terms of the range of both the initial membership and total masses of the simulated groups, which we fix to specific typical values (see below). In no case this latter constraint undermines the conclusions of this work.

2 SIMULATIONS AND METHODS

As part of a broader project aimed at studying galaxy merging in a realistic context, we have developed a high-resolution N -body model of a forming aggregation of galaxies which is a good and

computationally competitive approximation to pure cosmological experiments. Here we provide a summary of the main characteristics of this tool and the methodology adopted to analyse its outcomes, both discussed in great detail in Solanes et al. (2016; hereafter Paper I).

2.1 Group model

Our simulated groups start at redshift $z_i = 3$ as a (nearly) uniform, bound spherical overdensity initially expanding. Assuming that pressure gradients are negligible, a top-hat perturbation of amplitude $\delta_i > 0$ at the initial time t_i evolves like a Friedmann universe of initial radius given by

$$R_p(t_i) = \left[\frac{3M_p}{4\pi\rho_{\text{crit}}(t_i)\Omega_m(t_i)(1+\delta_i)} \right]^{1/3}, \quad (5)$$

where the suffix ‘p’ identifies quantities associated with the perturbation, i.e. the group, while the critical density, $\rho_{\text{crit}}(t_i)$, and the mass density parameter, $\Omega_m(t_i)$, refer to the unperturbed background cosmology – the contribution of the cosmological constant, Λ , to the evolution of the group can be neglected. For this work, we deal with simulated groups of total mass $M_p = M_{\text{tot, gr}} = 10^{13} h^{-1} M_\odot$ ($h \equiv H_0/100 \text{ km s}^{-1} \text{ Mpc}^{-1}$), with the value of the initial overdensity, δ_i , chosen so that a perfectly homogeneous top-hat perturbation of the same mass would collapse at $z = 0$. In our experiments, the time elapsed before turnaround, about 1/3 of the total simulation time of ~ 11.5 billion years in a standard concordant Λ CDM cosmology, serves for gravitational interactions between group members to build up peculiar velocities and n -point correlations among their positions, thus guaranteeing a reasonable approximation to a conventional galaxy group before merging becomes widespread during the non-linear gravitational collapse phase.

Each group region contains initially $N_{\text{gal}} = 25$ non-overlapping extended galaxy haloes. The total (virial) masses of this individual haloes, which obey a Navarro–Frenk–White density profile, are randomly drawn from a Schechter probability distribution function (pdf) of asymptotic slope $\alpha = -1.0$ and characteristic mass $M^* = 10^{12} h^{-1} M_\odot$. We set a lower limit in mass of $0.05 M^*$, as smaller haloes do not play a significant role in the results. For a given halo mass, the remaining global parameters of the dark haloes are fully determined by the background cosmology given a time of observation ($z_{\text{obs}} \simeq 0$). A 5 per cent of the total mass of each halo is placed in a stellar (baryonic) core following either a disc-bulge or a pure spheroidal distribution. Galaxies with masses less than $0.1 M^*$ are assumed for simplicity to host only spheroidal stellar distributions. Above this mass threshold, galaxy morphologies are established using a Monte Carlo technique that assumes a late-type galaxy fraction of 0.7. The initial structural and dynamical properties of all central stellar distributions are set so that they are consistent with the main local scaling laws defined by real objects of the same class. For late-type galaxies, disc scale-lengths, R_d , are initialized according to the analytic formalism for disc formation developed by Darriba & Solanes (2010), which relies on specific angular momentum conservation during gas cooling and adiabatic halo response to gas inflow. According to this model, which produces discs consistent with the local Tully–Fisher relationship calculated by Masters et al. (2006), R_d is equal to the virial radius of the parent halo times a factor expressed in terms of elementary functions that, for a given halo profile, depends on the values adopted for the halo concentration, c , spin parameter, λ , and stellar mass fraction, f_* (see Darriba & Solanes 2010 for a full account of the scaling methodology). On the other hand, and given that the adiabatic-gas-inflow

model is not very suitable for classical early-type galaxies, we set up such objects by directly relating their size measure, represented by the effective radius of their projected luminosity profiles, R_e , to their total mass, M , via the empirical formula

$$R_e = 2.05 \left[\frac{M}{M^*} \right]^{5/8} h^{-1} \text{ kpc.} \quad (6)$$

This scaling matches the observed size–luminosity relation for Sloan Digital Sky Survey (SDSS) spheroids reported by Bernardi et al. (2003) in the i^* -band if one assumes $f_* = 0.05$, a fixed rest-frame mass-to-light ratio Υ_I of 2.90 h solar units, and a colour equation ($i^* - I$) = 0.53 mag (Fukugita, Shimasaku & Ichikawa 1995). Equation (6) is also consistent with the R_e – M_* relation inferred by Shen et al. (2003).

After setting the central discy and spheroidal distributions of the progenitor galaxies, we scale down the total masses and taper radius of their dark haloes to values consistent with the initial redshift of the simulations. The stellar cores, however, are left unchanged given that in our experiments most mergers take place at a relatively late epoch in which the properties of galaxies are rather similar to those in the local volume. Once all the galactic haloes of a given group have been generated and rescaled, the common uniform background of the group is evenly filled with DM particles (identical to those that make the individual haloes) until a total group mass (dark plus luminous) of $10 M^*$ is reached. The initial positions of background particles (including the centre of mass of member galaxies) are randomly distributed inside the group volume, while their initial velocities follow the local Hubble flow.

2.2 Analysis of simulation data

A total of 48 groups have been created following the procedure just described. In order to compare mock and real data, we have projected the 3D spatial information contained in the final snapshot of each run on to the three Cartesian planes and, after adding a minimum sky background to all images, smoothed them with an isotropic kernel. We then have used the software SExtractor (Bertin & Arnouts 1996) to build a catalogue of group members. The global properties of the brightest group galaxies (BGGs) and of its lesser companions have been calculated from the three independent projected final images resulting from each simulation. This has allowed us to triple the sample size, offering at the same time a crude but useful information on the variance in the simulated data arising from object identification, projection effects and contamination by foreground companions. Further details on the description of the methodology adopted to process our simulations can be found elsewhere (Paper I).

For each group central remnant we have considered estimators of the basic global properties of size, internal velocity dispersion and scale, respectively represented by the half-stellar mass or effective radius, R_e , the mean stellar velocity dispersion within R_e , σ_e , and in the latter case indistinctly by either M_* , the total stellar mass, or by $\mu_e \equiv -2.5 \log[I_e] = -2.5 \log[(M_*/2)/(\pi R_e^2)]$, the mean stellar mass surface density within R_e . The use of the effective surface density in the definition of the FP makes this flat surface essentially independent of scale, because for spherically symmetric virialized systems its three dimensions are proportional to $M^{1/3}$. Another advantage of μ_e is that it is a proxy for the mean surface brightness from old stars – measured in a near-infrared window of the electromagnetic spectrum, such as the K -band – a distance-independent property (for nearby objects) preferred by observers.

3 RESULTS AND DISCUSSION

In Fig. 1 we provide a 3D graphical representation of the orthogonal (stellar mass) FP defined by our mock first-ranked group galaxies in the global parameter space [$\log R_e$, $\log \sigma_e$, μ_e]. The equation of the best-fitting orthogonal regression model is

$$\log R_e = (1.60 \pm 0.05) \log \sigma_e + (0.75 \pm 0.02) \mu_e / 2.5 - (8.0 \pm 0.2), \quad (7)$$

which is tilted relative to the standard plane defined by virialized systems that are homologous in a broad sense (see the Introduction). Quoted confidence intervals are median absolute deviations from 4000 bootstraps. In this figure we also plot the homogenized K -band data (see Paper I) from four different public compilations of massive hot spheroidal systems: a homogeneous set of 85 BCGs, the cluster counterparts of BGGs, with redshift z less than 0.1 extracted from the C4 cluster catalogue (Liu et al. 2008), the recently compiled catalogue of ETGs in clusters Norma and Coma by Mutabazi et al. (2014), the 6dFGS Fundamental Plane (6dFGSv) catalogue of nearly 9000 ETGs in the local ($z < 0.055$) Universe (Campbell et al. 2014), and a sample of 1, 430 ETGs in the redshift range 0.05–0.095 which combines photometric data from the SDSS and the UKIRT Infrared Deep Sky Survey (UKIDSS) (La Barbera et al. 2008). The FP delineated by our simulated remnants matches perfectly well not just the mean tilt, but also the normalization of the relatively narrow, flat 3-space region defined by the observations, all without requiring that progenitor galaxies have gas. This can be better visualized in Fig. 2 which compares the predicted values for each variable defining the inferred FP with the actual measurements. The lack of a clear non-random structure in the distribution of residuals is a sign that the model FP fits all the observations well. A collateral result of this analysis is the identification of a set of completely independent data bases of giant ellipticals with fully compatible measurements despite the not too insignificant differences which affect the selection and treatment of the data. This comes on top of recent claims that the FP of massive galaxies does not vary with environment, redshift or even star formation activity (La Barbera et al. 2008; Magoulas et al. 2012; Bezanson et al. 2015). The successful reproduction of the tilted FP relation is in sharp contrast with former dissipationless merger experiments that, with a few exceptions (Aceves & Velázquez 2005; Taranu et al. 2015), have systematically produced remnants which occupy a FP similar to that expected from virialized homologous systems. To our knowledge, ours is the most accurate experimental prediction of this basic relationship, regarding both its three coefficients and its reduced thickness, ever inferred from a numerical simulation of any kind aimed at studying the formation of the most massive galaxies in the Universe.

Another notable feature of the FP is that different classes of giant ETGs occupy distinctive areas on its surface, reflecting diversity in the structural and kinematic properties related to their respective formation histories (Faber et al. 1997; Bernardi et al. 2007; Bezanson et al. 2015). First-ranked galaxies are clearly segregated from the locus of the general population of giant ellipticals because of their considerably lower surface stellar mass density/brightness (Méndez-Abreu et al. 2012), whereas second-ranked objects lie on an intermediate position – being mindful that in simulations the recovering of galaxy properties degrades with decreasing brightness, we have found that mock galaxies with lower ranks depart progressively from the FP. Calculation of the vectors defined by the most important physical processes ruling the formation of hot stellar systems (energy dissipation, dissipationless mergers, mass loss through

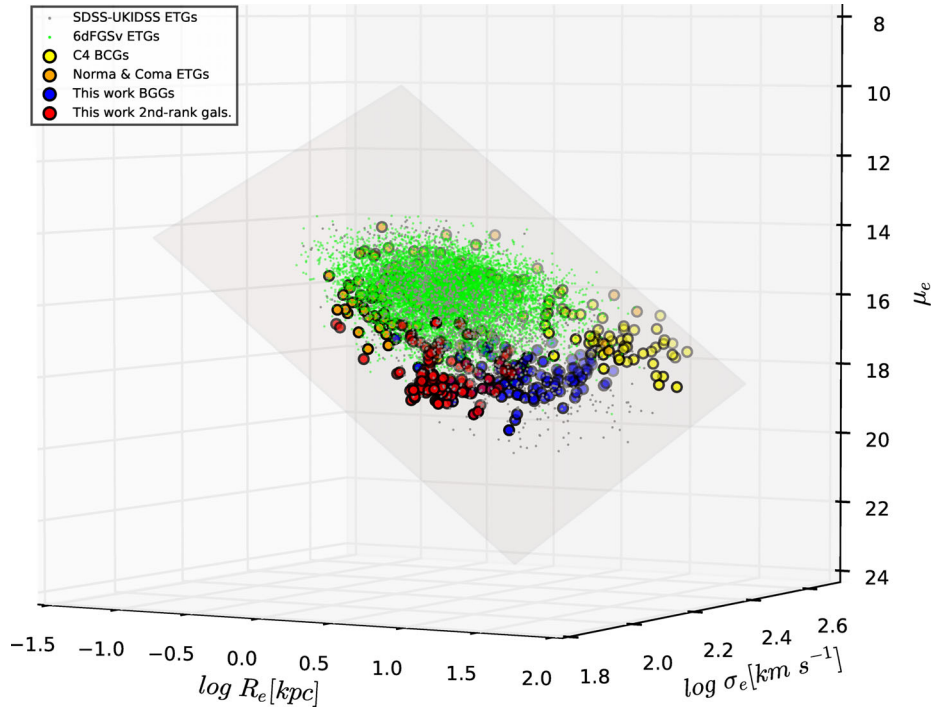


Figure 1. The tilted FP of massive hot spheroids. 3D graphical representation of the FP (light-grey plane) defined by our mock first-ranked group galaxies (big dark-blue circles) in the space of parameters $[\log R_e, \log \sigma_e, \mu_e]$. The distribution of our less reliably resolved second-ranked galaxies is also shown (big red circles), together with four published data sets of nearby ETGs: a homogeneous set of 85 BCGs extracted from clusters (big yellow circles), the ETGs in the Norma and Coma clusters (big orange circles), the 6dFGSv catalogue (green dots), and a volume-limited sample of ETGs based on SDSS-UKIDSS observations (small grey circles). Details on the transformations between simulated and observed measurements in this and the following figures can be found in Paper I. All subsets included in the plot show a strikingly similar tilt and normalization. Note also that we do not draw error bars in our measurements, but plot instead three independent points for each remnant corresponding to estimates along the Cartesian axes.

either supernova-driven winds or tidal and ram pressure stripping, etc.) in the full three-space of the FP, have shown that they move galaxies within the plane far more than they move them out of it (Bender et al. 1992). This provides a plausible explanation for the remarkable fact that in said space the common manifold of giant ETGs forms quite a slender sheet despite the strong stochasticity of the galaxy formation process. Fig. 2 also shows that the scatter around the FP is similarly connected to the ETG class, becoming smaller for classes with more massive representatives (this statement is reflected in quantitative terms in table 3 of Paper I). The reduced scatter of Liu et al. (2008)’s BCG data set, surpassed only by the even lower dispersion shown by our simulated galaxies, is another manifestation of the important regularity in the formation process of the most massive hot spheroids in the Universe which, according to our experiments, can be driven by purely gravitational phenomena.

The results outlined here, in harmony with other investigations of stochastic collisionless merging (Taranu et al. 2015), demonstrate that this mechanism is perfectly capable of reproducing the tight local relations that show the most fundamental parameters of these systems. It appears then that a realistic merger hierarchy can naturally provide the conditions required to reproduce the small intrinsic scatter shown by the observed stellar-mass scaling laws of massive ETGs without the need for a high degree of fine tuning between progenitors’ mass ratios and merger orbital parameters (Nipoti et al. 2009). In particular it should be noted that our progenitor galaxies have virial masses randomly drawn from a wide range of a Schechter pdf and initial positions that are uniformly distributed inside the group volume. Furthermore, the fact that we

simulate groups that are in the making implies that their member galaxies move most of the time in a mean gravitational field that is widely fluctuating and erratic because of the violent relaxation of the parent system. As a result, the outcome of the mergers that take place in such a highly non-linear phase – more specifically, the statistical distribution of the properties of the remnants – gets largely detached from the initial orbital characteristics of progenitor galaxies.

The fact that all massive ETGs fall into a single FP, coupled with the segregation of the highest ranked objects from lesser galaxies, entails that any non-edge-on projection of this flat surface must also lead to segregated 2D scaling laws. To investigate this issue we now use M_* to represent scale, shifting to the (logarithmic) *RVM* coordinate system defined by the three most basic global parameters connected by the standard plane. In this manner we set the framework for the study of two of the most firmly established empirical scaling relations of elliptical galaxies: the Kormendy-like *RM* relation (Shen et al. 2003) and the *VM* relation, a mass analogue of the classical FJR. In good agreement with observational studies of BCG/BGGs (Bernardi et al. 2007; Lauer et al. 2007; Bernardi 2009; Méndez-Abreu et al. 2012), we find that our simulated first-ranked galaxies lie off the standard 2D scaling relations defined by the bulk of the ETG population. In particular, as shown in Fig. 3, BGGs are larger and have lower effective velocity dispersions than ordinary ellipticals of the same stellar mass. The combination of this latter result with the fact that light appears to be similarly concentrated for BGGs than for non-BGGs (Paper I), tells us that the total mass-to-light fraction interior to R_e is lower for the former than for the latter. Our numerical experiments, however, do not seem to support

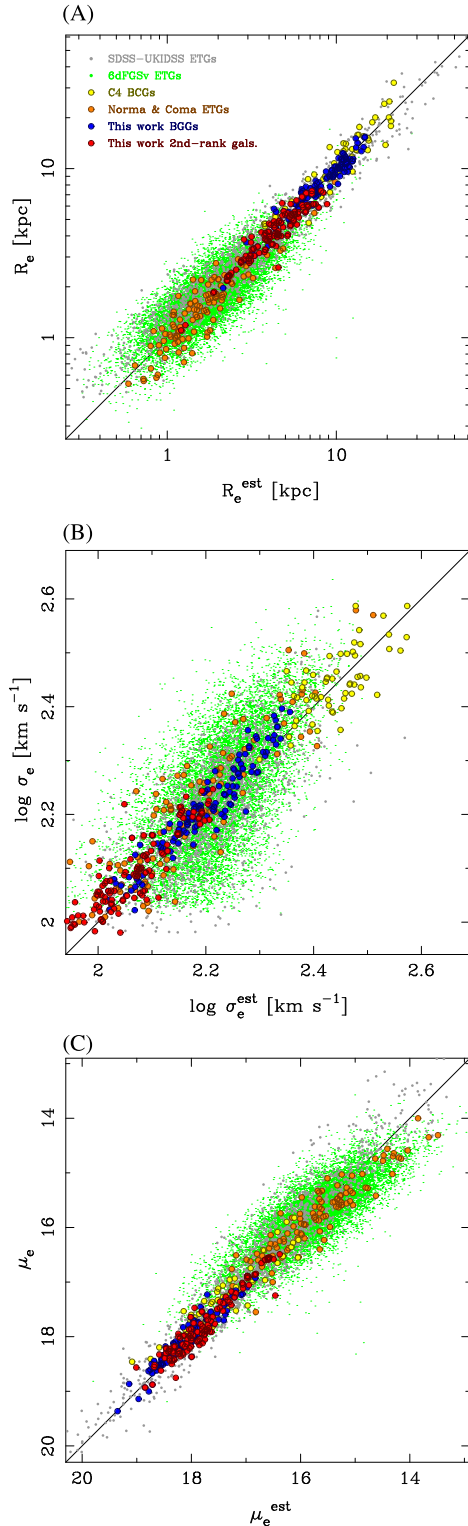


Figure 2. Residuals of FP fitting along the dimensions of the standard plane. From top to bottom: (A) R_e , (B) σ_e , and (C) μ_e . Data symbols are the same used in Fig. 1. In all panels the black diagonal line represents perfect agreement between real (Y axis) and estimated (X axis) values. The reasonably neutral behaviour of the residuals confirms that the model FP fits the observations well. Note that the samples containing the brightest objects, both simulated and observed, systematically show the smallest differences between expectations and measurements.

claims of the steepening of the $R \propto M^\alpha$ relation for CGs towards values $\alpha \gtrsim 1$ (Lauer et al. 2007; Bernardi 2009). We find instead that our first-ranked objects, which occupy a locus moderately offset from the central axis of the observational data in Fig. 3A, are well fitted by a model with $\alpha = 0.60 \pm 0.03$. This value of the power-law index agrees well with the slope $\alpha \sim 0.65$ found for non-BCG galaxies in the Sloan r -band (Shen et al. 2003; Bernardi et al. 2007), while a plain orthogonal fit to the general elliptical population data included in Fig. 3A (green dots and small grey circles) also gives $\alpha \sim 0.6$. Approaching closer to our findings, Liu et al. (2008) obtain $\alpha \sim 0.9$ from surface measurements up an isophotal limit of 25 r -mag arcsec $^{-2}$, which reduces to ~ 0.8 when their magnitudes are transformed into mass in old stars, whereas they get $\alpha \sim 0.75$ for a control sample of non-BCGs. Differences in the photometry, the waveband of the observations, sample construction (i.e. incompleteness and selection biases), and fitting methods would help explain the lack of a closer agreement between these results about the most robust of the 2D relationships.

The different locations of massive and regular ETGs along the FP also have a bearing on the zero-point of the $M \propto \sigma^\beta$ relation leaving, as in the previous case, the power law index hardly affected. The joint VM distribution (Fig. 3B) evidences that our simulated first-ranked galaxies have excess stellar mass above the prediction of the standard FJR, defining a roughly parallel sequence ~ 1.6 mag brighter (more massive) whose upper boundary extends into the area occupied by the BCGs’ data. This large intercept offset implies that, while the RM relation is basically an edge-on projection of the mass FP, the baryonic FJR is definitely not. Besides, it may also help to explain why the values of the slope of the FJR recovered from data sets that include a mix of BCGs and non-BCGs are considerably steeper than the canonical $\beta = 4$ (e.g. Lauer et al. 2007). In the current case, we find $\beta = 3.74 \pm 0.14$ from an orthogonal fit to the subset of our mock first-ranked galaxies. This value is consistent with most measurements reported in the literature (Kormendy & Djorgovski 1989; Pahre, Djorgovski & de Carvalho 1998; Kochanek 2006).

Fig. 3C displays the joint distribution of R_e and σ_e , which shows the FP almost face-on, providing a clear view of the almost non-existent correlation shown by these two variables – illustrating the general intransitivity of correlations – as well as of the substantially different areas occupied by central and non-central ETGs. This plot also best illustrates the moderate overlap shown by the point clouds corresponding to our simulated BGGs and their observational counterparts. This discrepancy can be ascribed to the fact that our mock first-ranked galaxies probably represent the lowest mass objects of its class – not all of them, for instance, are truly massive: $M_* > 10^{11} M_\odot$ – since these are central remnants assembled in isolated small groups rather than in the considerably larger galaxy aggregations hosting the bulk of the observed CGs. Indeed, as shown in the different panels of Fig. 3, the data points encircled in black corresponding to five of our largest simulated BGGs (the most fossil-like objects), as well as to the three CGs of the Norma and Coma clusters, fall squarely into the observed BCGs’ region (big yellow dots) – although on opposing sides – indicating that they all share similar characteristics. Pending that we extend this analysis to more massive galaxy aggregations, a good way to substantiate the proposed explanation is by taking advantage of the fact that our simulations are nominally scale-free, as long as our preferred transformations to physical units adopted in the initial setup continue to be acceptable. Thus, we have used the standard $R \sim V \sim M^{1/3}$ scaling verified by virialized spherical systems to infer a rough estimate of the 2D correlations that are to be expected from

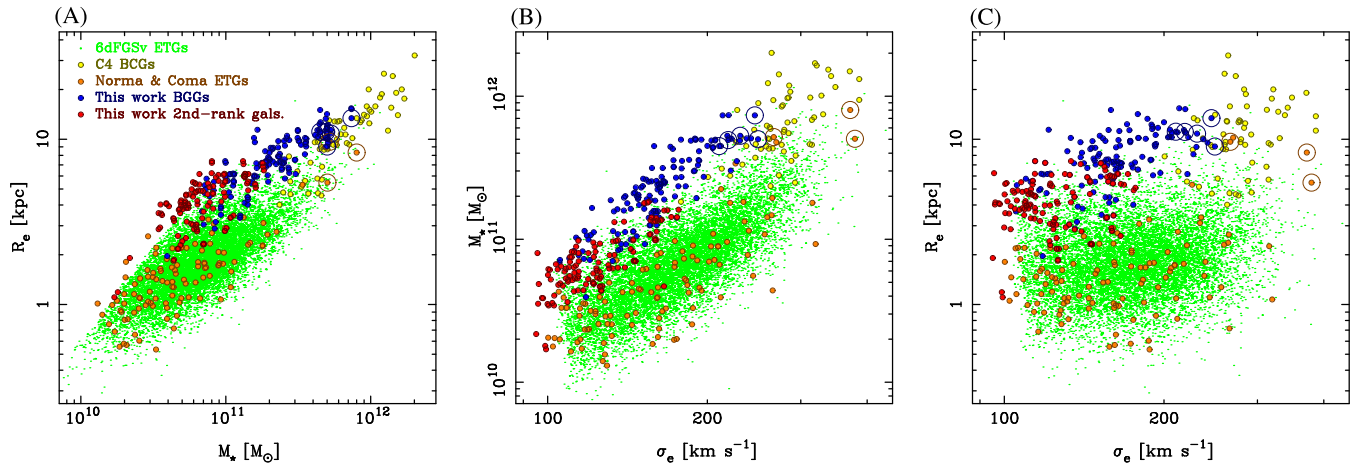


Figure 3. Projections of the FP in *RVM* space. (A) Size-stellar mass relation. (B) Stellar mass-velocity dispersion or mass FJR. (C) Size-velocity dispersion relation. Data symbols are the same used in Fig. 1 except for the SDSS-UKIDSS ETGs (La Barbera et al. 2008), which have not been included because they lack stellar mass information. The data points corresponding to our five simulated BGGs showing the largest magnitude gap between them and the second brightest group companion, as well as the three CGs of the Norma (1 object) and Coma (2 objects) clusters, are encircled. The positions of these very big objects in the FP projections are fully compatible with the point cloud of BCGs (big yellow circles).

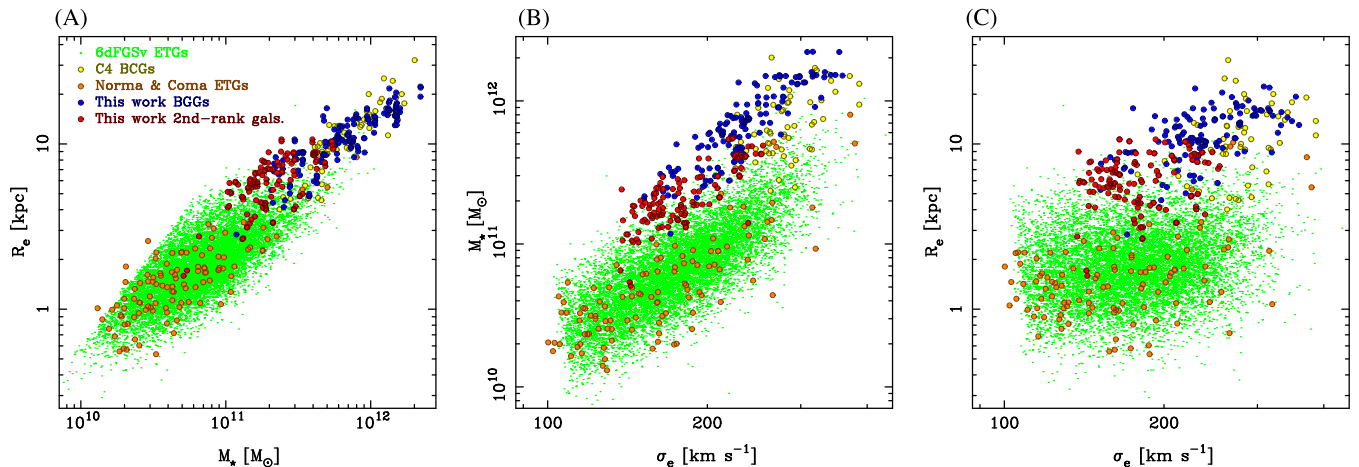


Figure 4. Predicted joint distributions of the properties of the brightest galaxies in more massive groups. Same as in Fig. 3 but after rescaling the properties of our simulated galaxies to the values expected when the mass unit of our simulations triples. The point clouds corresponding to our mock BGGs (big dark-blue circles) and the observed BCGs (big yellow circles) show now a substantial overlap in all three panels.

our simulations when, for instance, the mass of the host units triples (keeping N_{gal} constant). As depicted by Fig. 4, our predictions indicate that the global properties of simulated first-ranked galaxies of larger aggregations would match much better the volume occupied by Liu et al. (2008)’s BCGs in *RVM* space, showing a substantial overlap along all three projections. Interestingly, this would be accomplished virtually without changing the slopes of the relations delineated by the original data in Fig. 3 (as mentioned earlier, in $[R_e, \sigma_e, \mu_e]$ -space any re-scaling of the mass has a null impact on the FP coefficients).

Of all CG data sets used to date to investigate the scaling relations of these objects, that by Vulcani et al. (2014), based on an X-ray-selected sample of 169 groups at intermediate redshift ($z \sim 0.6$) and virial masses in the range $\sim [10^{13} - 10^{14}] M_{\odot}$, is among the most similar to ours in terms of the mass of the parent systems. Focusing again on comparisons mainly qualitative in nature, we find that the joint distributions of size and stellar mass of both BGG samples show a very good statistical agreement, in the sense that Vulcani et al. (2014)’s straight-line fits to their data also provide quite a rea-

sonably good description of our point cloud (Fig. 3A). In contrast, the other two relations involving the central velocity dispersion of galaxies show large offsets. The deviation is due to the fact that the intermediate- z BGGs have systematically higher values of σ_e (at fixed M_* or R_e) than their synthetic counterparts. It is, however, important to realize that the CGs in Vulcani et al. (2014) with a measured velocity dispersion constitute a magnitude-limited subset of the main sample. This biases their measurements against faint, low-stellar-mass objects, suggesting that the rescaled data from our Figs 4B and C would perhaps allow a more proper comparison. When doing so, we find indeed a substantial improvement in the overall consistency of the dynamic ranges in size, velocity and mass from both samples. Vulcani et al. (2014)’s study also brings out the fact that the late-time evolution of first-ranked galaxies eventually leads to changes in their global properties that largely involve a renormalization of the main 2D scaling laws that does not alter – or scarcely changes at worst – their slopes (compare their figs 10 and 11). This behaviour, analogous to that of the mass rescaling applied to our BGGs, suggests the stability of the FP with respect to the

secular evolution of CGs' properties, in good agreement with the theoretical predictions about the nature of this surface by Bender et al. (1992) and the observations by Bezanson et al. (2013).

4 CONCLUSION

Controlled hydrodynamical simulations of galaxy merging indicate that dissipation appears to be both necessary and sufficient to explain the tilt of the FP of ETGs (e.g. Robertson et al. 2006; Hopkins et al. 2008). This puts under strain observations of massive early-type objects claiming otherwise (Shen et al. 2003; Naab, Khochfar & Burkert 2006; Bernardi et al. 2007; Liu et al. 2008) and therefore the conjecture, advanced for more than a few years now by Kormendy (1989) and Bender et al. (1992), that ellipticals as a group constitute a continuum of merger-dominated systems in which the importance of gas in the outcome declines with increasing galaxy mass. It has to be noted, however, that the merger hierarchy typical of Λ CDM cosmologies has been traditionally recreated in numerical experiments through a sequence of two or three non-overlapping major binary collisions of homologous systems that use the remnants of one step to realize the initial conditions of the next (e.g. Dantas et al. 2003; Robertson et al. 2006; Nipoti et al. 2009; Moody et al. 2014). These idealizations of multiple merging can hardly capture the diversity of galaxy interactions that take place in the course of cosmic evolution, especially when it comes to the distribution of orbits, frequencies and mass ratios. In contrast, our cosmologically consistent simulations of pre-virialized galaxy associations provide the most convincing evidence presented to date on the viability of hierarchical collisionless merging as a formation channel for first-ranked objects through the reproduction of their main global properties and correlations, leading therefore to the removal of the last remaining obstacle for the experimental validation of the merger continuum conjecture.

ACKNOWLEDGEMENTS

We thank the referee, Carlo Nipoti, for his useful comments and suggestions. This work was supported by the Program for Promotion of High-Level Scientific and Technical Research of Spain under projects AYA2010-15169 and AYA2013-40609-P.

REFERENCES

Aceves H., Velázquez H., 2005, *MNRAS*, 360, L50
 Beifiori A. et al., 2014, *ApJ*, 789, 92
 Bender R., Burstein D., Faber S. M., 1992, *ApJ*, 399, 462
 Bernardi M., 2009, *MNRAS*, 395, 1491
 Bernardi M. et al., 2003, *AJ*, 125, 1866
 Bernardi M., Hyde J. B., Sheth R. K., Miller C. J., Nichol R. C., 2007, *AJ*, 133, 1741
 Bertin E., Arnouts S., 1996, *A&A*, 317, 393
 Bezanson R., van Dokkum P. G., van de Sande J., Franx M., Leja J., Kriek M., 2013, *ApJ*, 779, L21
 Bezanson R., Franx M., van Dokkum P. G., 2015, *ApJ*, 799, 148
 Campbell L. A. et al., 2014, *MNRAS*, 443, 1231
 Cappellari M. et al., 2013, *MNRAS*, 432, 1862
 Carlberg R. G., 1986, *ApJ*, 310, 593
 Ciotti L., 1997, in Renzini A., da Costa L. N., eds, *Galaxy Scaling Relations: Origins, Evolution and Applications*. Springer-Verlag, Berlin, p. 38
 Ciotti L., Lanzoni B., Volonteri M., 2007, *ApJ*, 658, 65

Cox T. J., Dutta S. N., Di Matteo T., Hernquist L., Hopkins P. F., Robertson B., Springel V., 2006, *ApJ*, 650, 791
 Dantas C. C., Capelato H. V., Ribeiro A. L. B., de Carvalho R. R., 2003, *MNRAS*, 340, 398
 Darriba L., Solanes J. M., 2010, *A&A*, 516, A7
 De Lucia G., Blaizot J., 2007, *MNRAS*, 375, 2
 Djorgovski S., Davis M., 1987, *ApJ*, 313, 59
 Dressler A., Lynden-Bell D., Burstein D., Davies R. L., Faber S. M., Terlevich R., Wegner G., 1987, *ApJ*, 313, 42
 Eggen O. J., Lynden-Bell D., Sandage A. R., 1962, *ApJ*, 136, 748
 Emsellem E. et al., 2007, *MNRAS*, 379, 401
 Faber S. M., Jackson R. E., 1976, *ApJ*, 204, 668
 Faber S. M. et al., 1997, *AJ*, 114, 1771
 Fukugita M., Shimasaku K., Ichikawa T., 1995, *PASP*, 107, 945
 Hoffman L., Cox T. J., Dutta S., Hernquist L., 2010, *ApJ*, 723, 818
 Hopkins P. F., Cox T. J., Hernquist L., 2008, *ApJ*, 689, 17
 Huertas-Company M. et al., 2013, *MNRAS*, 428, 1715
 Kochanek C. S., 2006, in Meylan G., Jetzer P., North P., eds., *Saas-Fee Advanced Course Num. 33*. Springer-Verlag, Berlin, p. 91
 Kormendy J., 1977, *ApJ*, 218, 333
 Kormendy J., 1989, *ApJ*, 342, L63
 Kormendy J., Djorgovski S., 1989, *ARA&A*, 27, 235
 La Barbera F., Busarello G., Merluzzi P., de la Rosa I. G., Coppola G., Haines C. P., 2008, *ApJ*, 689, 913
 La Barbera F., de Carvalho R. R., de La Rosa I. G., Lopes P. A. A., 2010, *MNRAS*, 408, 1335
 Lauer T. R. et al., 2007, *ApJ*, 664, 226
 Liu F. S., Xia X. Y., Mao S., Wu H., Deng Z. G., 2008, *MNRAS*, 385, 23
 Magoulas C. et al., 2012, *MNRAS*, 427, 245
 Masters K. L., Springob C. M., Haynes M. P., Giovanelli R., 2006, *ApJ*, 653, 861
 Méndez-Abreu J. et al., 2012, *A&A*, 537, A25
 Moody C. E., Romanowsky A. J., Cox T. J., Novak G. S., Primack J. R., 2014, *MNRAS*, 444, 1475
 Mutabazi T., Blyth S. L., Woudt P. A., Lucey J. R., Jarrett T. H., Bilicki M., Schröder A. C., Moore S. A. W., 2014, *MNRAS*, 439, 3666
 Naab T., Khochfar S., Burkert A., 2006, *ApJ*, 636, L81
 Nipoti C., Londrillo P., Ciotti L., 2003, *MNRAS*, 342, 501
 Nipoti C., Treu T., Auger M. W., Bolton A. S., 2009, *ApJ*, 706, L86
 Novak G. S. 2008, PhD thesis, Univ. of California
 Oser L., Ostriker J. P., Naab T., Johansson P. H., Burkert A., 2010, *ApJ*, 725, 2312
 Ostriker J. P., 1980, *Comments Astrophys.*, 8, 177
 Padmanabhan N. et al., 2004, *New Astron.*, 9, 329
 Pahre M. A., Djorgovski S. G., de Carvalho R. R., 1998, *AJ*, 116, 1591
 Robertson B., Cox T. J., Hernquist L., Franx M., Hopkins P. F., Martini P., Springel V., 2006, *ApJ*, 641, 21
 Shen S., Mo H. J., White S. D. M., Blanton M. R., Kauffmann G., Voges W., Brinkmann J., Csabai I., 2003, *MNRAS*, 343, 978
 Solanes J. M., Perea J. D., Darriba L., García-Gómez C., Bosma A., Athanasoulas E., 2016, *MNRAS*, 461, 321 (Paper I)
 Taranu D. S., Dubinski J., Yee H. K. C., 2013, *ApJ*, 778, 61
 Taranu D. S., Dubinski J., Yee H. K. C., 2015, *ApJ*, 803, 78
 Toomre A., 1977, in Tinsley B. M., Larson R. B., eds, *Evolution of Galaxies and Stellar Populations*. Yale University Observatory, New Haven, p. 401
 Toribio M. C., Solanes J. M., Giovanelli R., Haynes M. P., Martin A. M., 2011, *ApJ*, 732, 93
 Trujillo I., Ferreras I., de La Rosa I. G., 2011, *MNRAS*, 415, 3903
 Vulcani B. et al., 2014, *ApJ*, 797, 62
 Weil M. L., Hernquist L., 1996, *ApJ*, 460, 101

This paper has been typeset from a $\text{\TeX}/\text{\LaTeX}$ file prepared by the author.